Journal of Precision Instrument and Machinery (2025)
Clausius Scientific Press, Canada

DOI: 10.23977/jpim.2025.050105
ISSN 2616-1990 Vol. 5 Num. 1

Heat and Mass Transfer Study during the Reduction of Iron Ore Pellets in a Fixed-Bed Reactor

Chang Xu[1,*], Jian Pan[2], Congcong Yang[2], Haibin Yang[1]

[1]*Lodestone Technology Co., Ltd., Shanghai, China*
[2]*School of Minerals Processing and Bioengineering, Central South University, Changsha, 410083, China*
[*]*Corresponding author*

Keywords: Fixed Bed Reactor; Computational Fluid Dynamics; Iron Ore Pellet Reduction; Heat and Mass Transfer Coupling; Hydrogen Metallurgical Process Optimization

Abstract: As the pressure of the "dual carbon" target in the steel industry intensifies, the hydrogen-based direct reduction (H_2-DR) process has become a key path for green and low-carbon ironmaking due to its significant emission reduction potential. However, the existing process lacks intelligent perception and control capabilities, and cannot accurately grasp the gas-solid heat and mass transfer state in the fixed bed reactor, which limits the reduction efficiency and energy consumption optimization level. To this end, this paper combines computational fluid dynamics (CFD) technology with reaction kinetics modeling methods to construct a numerical model of heat transfer-mass transfer-reaction coupling in the hydrogen reduction pellet process, and conducts high-precision simulation analysis of key parameters such as gas composition ($H_2/CO/N_2$), temperature, flow rate, and pellet stacking structure. This paper simulates three typical hydrogen concentration conditions (H_2 100%, 80%, 60%) through a two-dimensional axisymmetric model, couples the RNG k-ε turbulence model with the $Fe_2O_3 \rightarrow Fe$ reduction path, and combines the porous medium model to calculate the heat and mass transfer of the stacked pellet bed. The changes in the temperature field, velocity field and mole fraction distribution of the gas in the reactor are comprehensively analyzed, and the heat transfer efficiency, gas dissipation path and rate control link of the reduction zone are accurately identified. The results show that under the operating temperature of 950 ℃ and the H_2 concentration of 82%, the temperature drop of the gas in the pellet bed reaches 80K, the H_2 mole fraction decreases by about 17%, and the reaction rate increases to 0.0524 $kmol/m^3s$, which is much higher than 0.0021 $kmol/m^3s$ under CO conditions.

1. Introduction

With the urgent need of the steel industry for low-carbon and high-efficiency metallurgical technology, the direct reduction process of iron ore pellets has become a key link in research and industrial practice. As an important raw material for blast furnaces and direct reduction devices, the reduction behavior of pellets is affected by multiple factors such as raw material properties, structural characteristics and reducing atmosphere. In recent years, a large number of studies have been carried out on the development of biomass reductants, the application of hydrogen-based reducing atmospheres, the evolution of pellet pore structures, and the optimization of organic binders, aiming to improve the metallurgical properties and environmental sustainability of pellets.

However, current research focuses on single variables, such as temperature, atmosphere or raw material composition, and lacks a systematic understanding of the synergistic effect of the structural evolution and reduction behavior of pellets throughout their life cycle, especially in terms of multi-parameter interaction, microstructure reconstruction and its correlation mechanism with macroscopic performance. In addition, in-depth exploration is still needed to build a reduction kinetics and structural evolution model with predictive capabilities to guide the design and optimization of high-performance pellets.

This study aims to integrate existing research results, systematically analyze the key factors affecting the pellet reduction process, including raw material quality, structural defects, atmosphere composition and temperature gradient, and combine experimental data with model establishment to reveal the coupling mechanism between the pellet reduction behavior and its structural evolution, providing a theoretical basis and technical support for the realization of low-carbon and high-efficiency pellet preparation and green steel manufacturing.

2. Related Work

In recent years, with the development of green metallurgical technology, low-carbon reduction paths and pellet performance optimization have become research hotspots. Many scholars have carried out systematic research on biomass substitution, hydrogen reduction, structural evolution and binder application, and achieved rich results, as described below.

Singh et al. characterized three biomasses (Acacia, Albizia Julibrissin, and Melaleuca Albizzia) and used their volatiles to reduce iron ore pellets at high temperature and produce charcoal at the same time. The study investigated the effects of different biomasses and reduction parameters on the reduction rate, with the highest reduction rate reaching 89% [1]. Das et al. used peanut shells and corn cobs containing high volatiles and charcoal prepared at 350 ℃ as reducing agents to reduce iron ore pellets. The results showed that the reduction rate of corn cob charcoal was as high as 92.01%, and the volatile reduction rate was 78.38% [2]. Wang et al. systematically analyzed the reduction behavior of hematite pellets with different iron grades in a hydrogen-containing reducing atmosphere and found that the appropriate pore size distribution (0.7–7 μm) had a greater effect on the reduction rate than the iron grade. The addition of hydrogen significantly reduced the activation energy and improved the reduction efficiency [3]. Kittivinitchnun et al. established a non-isothermal reduction kinetic model to simulate the reduction process of a single self-reduced iron ore pellet in the hot storage area of a blast furnace. The model took into account the effects of temperature, gas composition and pellet composition on the reduction kinetics of Fe2O3, Fe3O4 and FeO. Through the use of a set of ordinary differential equations and MATLAB numerical solutions, the model achieves the prediction of mass change and reduction degree[4]. Bersenev et al. analyzed the structural characteristics of iron ore pellets and their influence on metallurgical properties, pointing out that the pore properties and structural defects of the original pellets play a decisive role in the performance[5]. Mishra et al. used low-grade iron ore waste containing goethite to prepare high-grade iron ore pellets through reduction roasting and magnetic separation. The experiment adopted Taguchi L9 design and determined the optimal roasting conditions to be 900 ℃, 30 minutes, and the roasting recovery rate reached 84.2%[6]. Hessling et al. investigated the effect of water vapor partial pressure (0-15%) on the hydrogen reduction process (873K–1173K) of industrial hematite pellets. The results showed that water vapor significantly affected the reduction rate and pellet microstructure at low temperature of 873K, and the effect was weakened at high temperature[7]. Lyu et al. simulated the non-isothermal reduction of iron ore pellets under different atmospheres in the blast furnace block zone and analyzed the kinetic mechanism and micromorphology. The results showed that the reduction starting temperature changed under hydrogen enrichment conditions, and the reduction degree was significantly improved, up to 100%[8]. Avula et al. investigated the isothermal reduction behavior of low-grade Ramallakota and high-grade Bolani iron ore pellets in coke-free coal at 1123, 1173 and 1223 K. The reduction rate of Ramallakota pellets was better than that of Bolani due to their higher porosity and gangue content. XRD showed that Ramallakota was reduced more completely, and both produced pyrrhotite and spinel[9]. Bersenev et al. established a model to analyze the change in porosity of iron ore pellets from pelletization to complete reduction. The results showed that the pore volume of the pellets shrank slightly (2-5%) during high-temperature sintering, and the porosity increased by 100-200% to 46-60% due to expansion during the reduction process[10]. Claremboux and Kawatra reviewed the role of organic binders in the preparation of iron ore pellets. An effective organic binder must disperse the iron ore well, maintain dispersion and have a low water content. The advantage of organic binders is that they do not introduce silica, are used in small quantities, and are more readily available in some regions [11]. However, existing studies have mostly focused on the effects of a single factor on reduction behavior or performance, lacking a systematic revelation of the synergistic mechanism of multiple factors and a dynamic optimization model for the entire process.

3. Method

3.1 Fixed Bed Reactor Structure Modeling

In order to deeply analyze the heat and mass transfer behavior inside the reactor during the process of hydrogen reduction of iron ore pellets, this study established a three-dimensional geometric model of the fixed bed reactor based on the experimental platform, and combined the computational fluid dynamics (CFD) method for structural modeling and physical field simulation. The model not only covers the pellet accumulation area and gas flow space but also comprehensively considers the coupled processes of gas heating, diffusion, reaction, etc. in the reactor.

(1) Geometric structure and bed design

The fixed bed reduction furnace adopts a vertical cylindrical structure with an inner diameter of Φ76.2 mm. The pellet samples are placed in the center of the reaction chamber in a stacked state. The overall stacking height is about 150 mm. An axisymmetric two-dimensional model is constructed based on the experimental structure for simplification. To ensure the simulation accuracy, the pellet bed area is defined as a porous medium with a porosity of 20.8%, which is derived from the average porosity of the pellet samples measured in practice (19.93%~21.69%). The average particle size of the pellets in the bed is 10 mm, and the spatial arrangement of the particles is handled according to the uniform distribution assumption.

(2) Boundary condition setting

The following boundary conditions are set in the model:

Gas inlet (upper end): The velocity inlet boundary condition is adopted, and the gas volume fraction is set to two typical atmospheres of H_2:CO:CO_2:N_2 = 82:10:3:5 (coke oven gas) and 55:21:14:10 (HYL gas) according to the experimental conditions. The inlet temperatures are 1073 K,1123 K, 1173 K, and 1223 K for comparison;

Gas outlet (lower end): constant pressure outlet is used, and the outlet pressure is set to 101325 Pa to simulate the free discharge condition of gas;

Wall boundary: set to a constant wall temperature boundary. According to Figure 3-20, the wall temperature is controlled at the operating temperature (such as 800 ℃). The wall adopts a no-slip boundary condition (u = 0), ignoring radiation and external heat loss, and the heat transfer is mainly forced convection of the wall to the gas;

Initial conditions: the initial temperature in the reactor is set to the operating temperature, the gas is a mixed reducing gas component, and the reactant pellets are at room temperature (300 K) to simulate the heating process.

(3) Pressure drop and thermal resistance analysis parameters

The Ergun equation (see the literature formula) is introduced into the structural model to model the pressure drop in the pellet accumulation area. The specific formula is as follows:

$$\Delta P = \frac{150.(1-\varepsilon)^2.\mu.u}{\varepsilon^3.d_p^2} + \frac{1.75.(1-\varepsilon).\rho.u^2}{\varepsilon^3.d_p} \qquad (1)$$

Among them, ε is the bed porosity; μ is the gas viscosity; u is the gas velocity; d is the pellet size; and p is the gas density.

This model is used to estimate the flow resistance in a fixed bed and verify the rationality of the flow field and pressure drop in the simulation.

3.2 Construction of Gas Flow Field and Heat Transfer Environment

In order to reflect the heating and flow behavior under real industrial conditions, a dynamic gas heating process is introduced into the model: after the gas enters the reactor, it is heated along the wall, and a reduction reaction and temperature change occur while passing through the pellet accumulation area. As shown in Figure 1, the gas temperature has reached 700 ℃ at 1/2 of the reactor length and rises to the operating temperature near the bottom. This temperature distribution feature is accurately simulated by CFD calculation, capturing the effects of thermal convection and heat transfer non-uniformity on gas activity.

At the same time, the thermal resistance effect between particles is considered in the porous medium model, and the equivalent thermal conductivity is used to describe the heat transfer behavior inside the pellets. The thermal conductivity of the stacking area directly affects the heat transfer efficiency and reaction uniformity, providing a parameter basis for subsequent heat transfer optimization and structural adjustment.

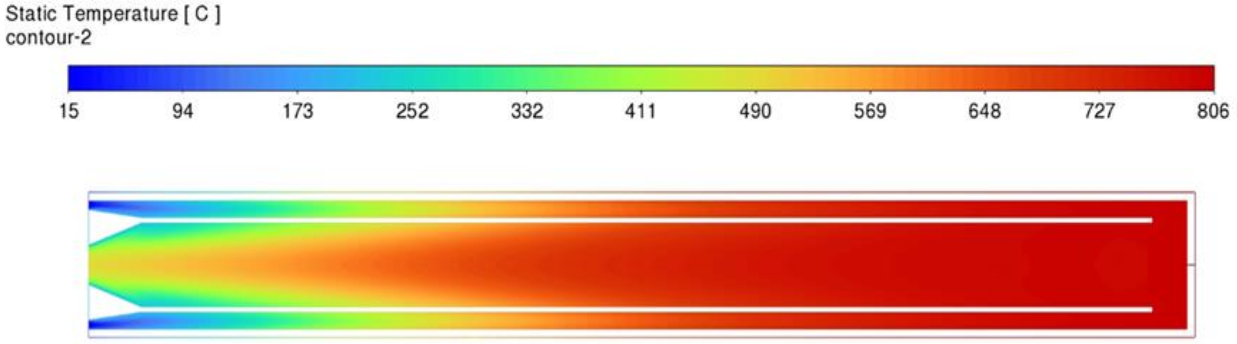

Figure 1 Gas temperature in the reduction furnace

4. Results and Discussion

In order to deeply understand the flow and reaction characteristics of multi-component gases in a fixed bed reactor during hydrogen reduction, this study used the CFD method to numerically simulate the gas flow field, temperature field and component concentration field. The simulation content covers different mixing ratios of hydrogen and nitrogen. Combined with actual atmospheres (such as coke oven gas and HYL gas), a gas-solid coupling reaction model is constructed to model the gradual reduction path of Fe_2O_3 to metallic iron (Fe), and its heat and mass transfer behavior is solved under porous media conditions.

(1) Comparison of gas component settings and operating conditions

Three groups of typical operating conditions are set in the simulation, corresponding to different hydrogen gas integral fractions to reflect the influence of changes in hydrogen concentration on heat and mass transfer behavior:

Table 1 Comparison of gas component settings and operating conditions

Case Number	Hydrogen Volume Fraction (vol.%)	Gas Composition (H_2/N_2)
Case 1	100%	H_2: 100%
Case 2	80%	H_2: 80%, N_2: 20%
Case 3	60%	H_2: 60%, N_2: 40%

In addition, corresponding to the actual experimental conditions, coke oven gas (COG) and HYL gas are used as reducing gases (as shown in Table 1) to further conduct component simulation and comparative analysis to verify the scalability and engineering applicability of the model.

(2) Gas flow model and turbulence processing

In the reactor, the gas flow process is in the low Reynolds number quasi-laminar region, especially in the porous packed bed area where the flow velocity is limited. In order to more accurately capture the flow characteristics, the RNG k-ε turbulence model is used in the simulation. This model can more effectively handle phenomena such as flow recirculation and boundary layer shear, and adapt to low turbulence behavior in complex structures.

The model takes into account the flow resistance effect of the porous medium region, and its viscosity and inertial resistance terms are derived from the bed porosity ε and the pellet size d_p, respectively. Specifically, the Ergun equation is embedded in the calculation flow field to simulate the real velocity distribution of the gas in the porous medium. Figures 2 and 3 show the velocity distribution of the gas inside the reactor and around the pellet bed. The flow velocity in the pellet area gradually decreases from 0.35 m/s at the inlet to 0.15 m/s, which is consistent with the velocity homogenization characteristics during the reaction process.

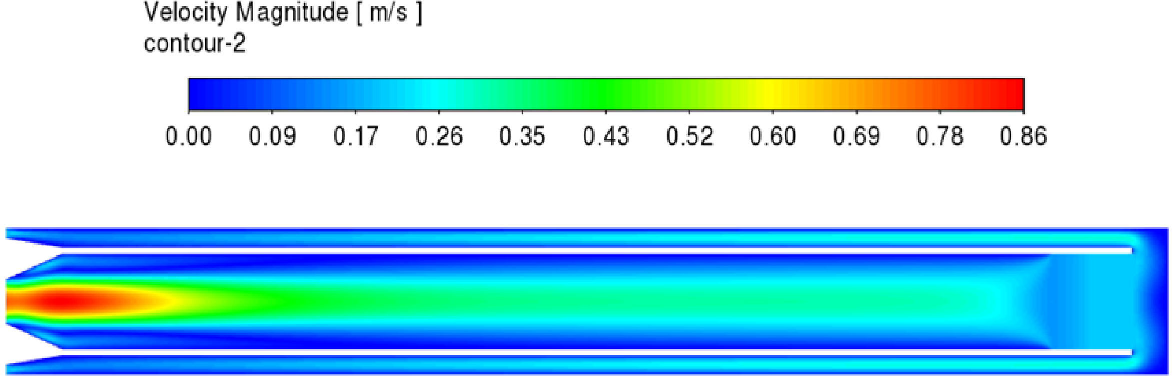

Figure 2 Gas velocity in the reduction furnace

Figures 2 and 3 show the velocity distribution of the gas in the mainstream area and the pellet accumulation area, respectively. In the mainstream area, the gas has a typical tube flow velocity distribution, with a central velocity of up to 0.86 m/s and a velocity close to 0 near the wall, showing obvious laminar characteristics. After entering the accumulation bed area, the gas velocity decreases significantly and tends to be uniform, with an average velocity of about 0.15 m/s, indicating that the porous resistance in the pellet area causes momentum dissipation.

Figure 3 further indicates that the gas velocity distribution inside the pellet accumulation area is narrow (0.12–0.18 m/s), but the velocity slightly increases at the upper and lower edges of the accumulation area, indicating that the boundary effect causes the existence of local "bypass" flow, which may affect the uniform reduction of the bed. It is necessary to introduce a guide structure or optimize the air intake distribution in the actual design.

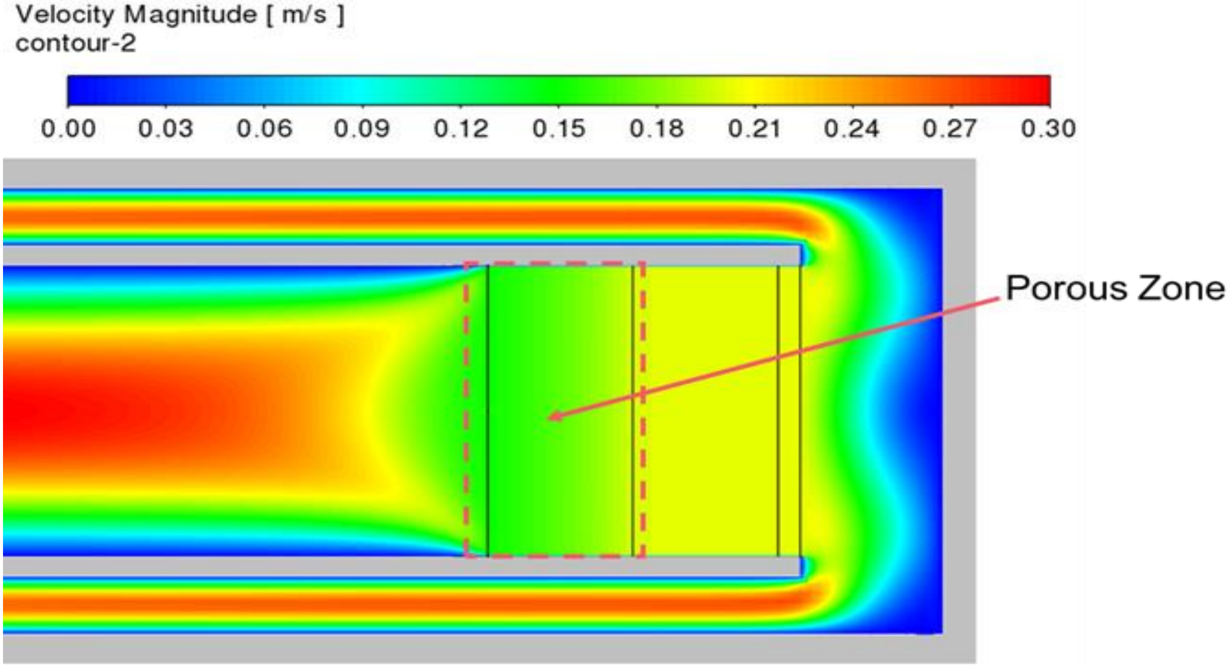

Figure 3 Gas velocity distribution around the accumulated pellets in the reduction furnace

(3) Kinetic model of reduction reaction

The gas-solid reaction process uses a simplified three-step reaction path to describe the iron-oxygen reduction process:

$$Fe_2O_3 \rightarrow Fe_3O_4 \rightarrow FeO \rightarrow Fe$$

Since there are two reducing agents, H_2 and CO, in the actual reaction system, in order to distinguish their reaction characteristics, the kinetic models of hydrogen reduction and carbon monoxide reduction are constructed, respectively. Based on the model proposed by A. A. El-Geassy et al. in ISIJ Transactions [1977], the parameters are corrected and the kinetic equation is as follows:

$$\mathrm{r} = \mathrm{A}.\mathrm{P}^{\mathrm{n}}\exp(-\frac{\mathrm{E}}{\mathrm{RT}}) \tag{2}$$

Among them, A is the pre-exponential factor; P is the gas partial pressure; E is the activation energy; R is the gas constant; T is the absolute temperature. The kinetic parameters are shown in Table 2. The activation energy of the hydrogen reduction reaction is significantly higher than that of CO, indicating that it is more sensitive to temperature.

Table 2 Kinetic parameters

Parameters	Unit	H_2	CO
Pre-exponential Factor	1/s bar	0.265	-0.232

Figure 4 shows the distribution of the reaction rate of the pellet bed with CO under different temperature conditions when coke oven gas (COG) is used as the reducing gas. The reaction rate is affected by temperature and the partial pressure of the reaction gas. Under this condition, the temperature and CO partial pressure inside the bed change little, so the reaction rate distribution remains basically constant. At 800 °C, the reaction rate of the pellet with CO is about 0.0015 kmol/m^3s. As the temperature rises to 950 °C, the reaction rate increases to 0.0021 kmol/m^3s. This increase in rate is mainly attributed to the fact that the increase in temperature accelerates the kinetic process of the reduction reaction. As can be seen from the figure, the reaction rate is relatively uniform in radial distribution, indicating that during the reduction reaction, the mass transfer resistance of CO in the pellet bed is small, and the gas can evenly penetrate the entire bed, ensuring the effective progress of the reaction.

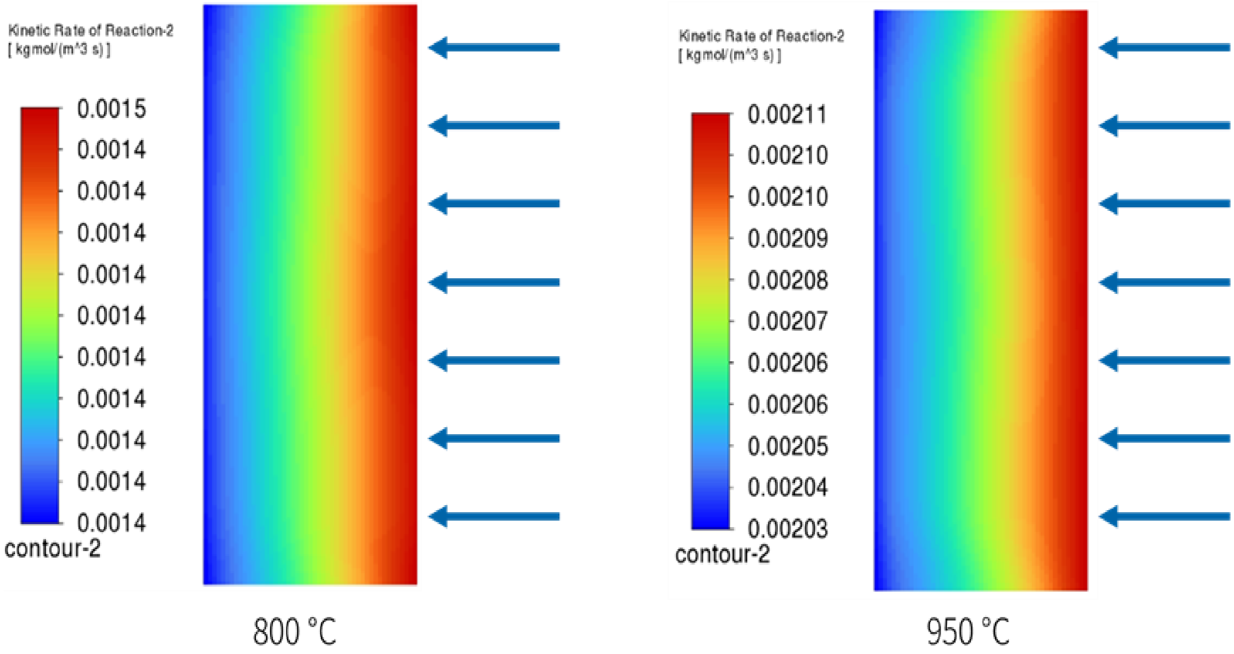

Figure 4 Distribution of reaction rates of COG with CO at different temperatures when used as a reducing gas

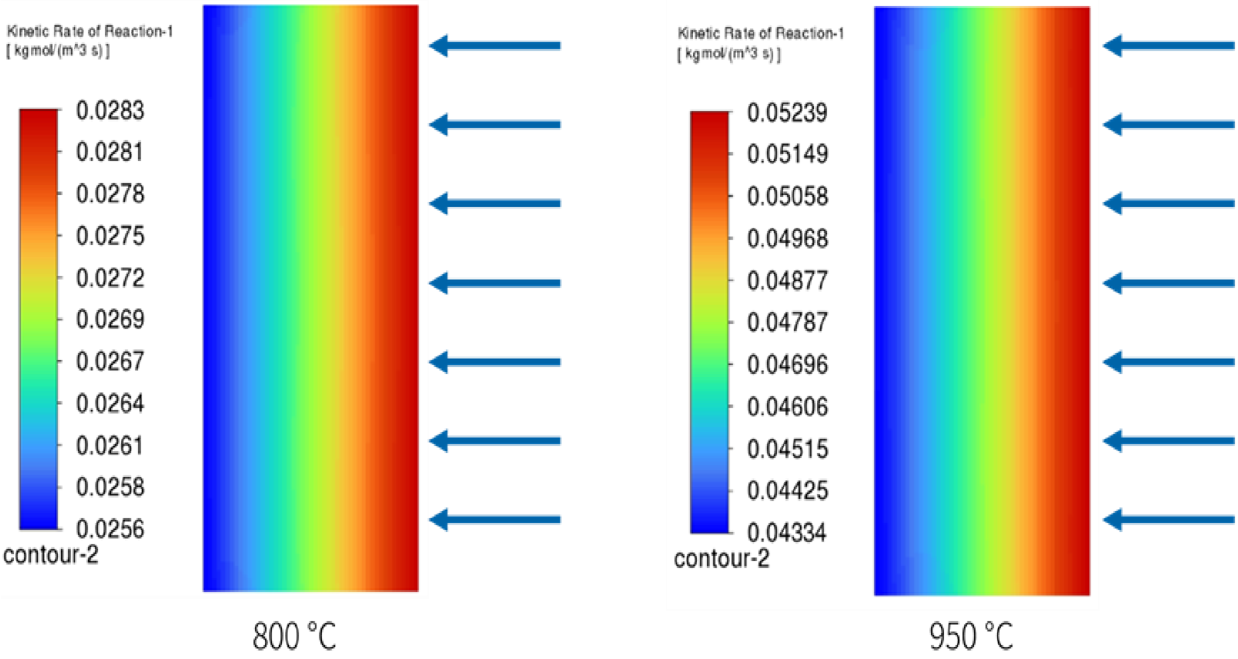

Figure 5 Distribution of reaction rates of COG with H2 at different temperatures when it is used as a reducing gas

The hydrogen reaction rate reaches 0.0283 $kmol/m^3s$ at 800 ℃ (inlet) and drops to 0.0256 $kmol/m^3s$ at the outlet; while the CO reduction reaction rate increases from 0.0015 $kmol/m^3s$ to 0.0021 $kmol/m^3s$ (at 950 ℃) (as shown in Figures 4 and 5).

(4) Solver and numerical settings

This study uses COMSOL Multiphysics 6.0 and ANSYS Fluent 2023R1 for verification and flow field/reaction simulation. During the numerical solution process:

Solver: SIMPLE algorithm based on pressure coupling;

Spatial discretization: second-order upwind scheme;

Chemical species transport: convection + diffusion + reaction source terms are considered;

Gas model: ideal gas, temperature-dependent properties are fitted from experimental data in the literature;

Initial field: flow velocity 0, temperature distribution is set to isothermal or linear variation field.

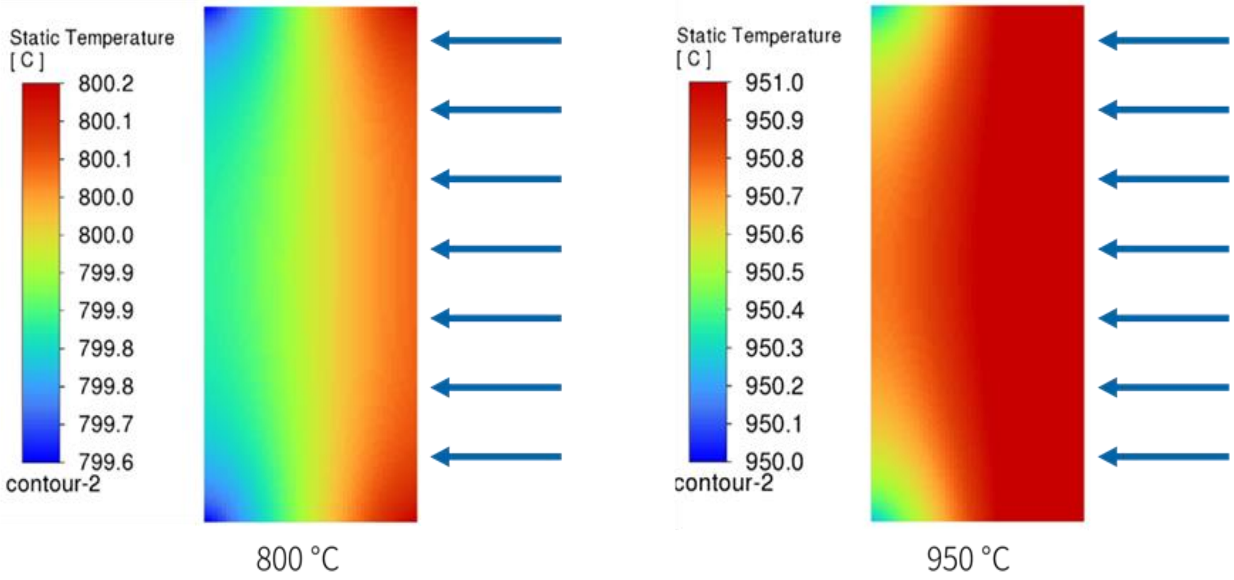

Figure 6 Temperature distribution inside the sample at different temperatures when COG is used as the reducing gas

A 2D axisymmetric structure is used, with about 60,000 grids. The model calculation stability is verified by grid independence analysis. The model results are shown in Figures 6 and 7, showing the distribution of gas composition (H_2, CO) and temperature in the pellet accumulation area at different temperatures, revealing the evolution mechanism of the mass transfer-reaction-heat coupling process.

Figures 7 and 8 show the mole fraction distribution of CO and H_2 inside the pellet bed, respectively, revealing the attenuation characteristics of gas concentration along the reaction path.

CO: The initial mole fraction is 0.1, which drops to 0.097 at the outlet at 800 ℃ and 0.096 at 950 ℃, with a small change range, indicating that the CO reaction rate is slow and has low temperature dependence;

H_2: The initial mole fraction is 0.82, which drops to 0.74 at the outlet at 800 ℃ and 0.68 at 950 ℃,with a decrease of 17%, indicating that H_2 is consumed rapidly in the bed, the reduction reaction is intense, and it has good permeability and mass transfer capacity.

Overall, the concentration distribution of the two reducing gases in the pellet area is relatively uniform, and the radial gradient is not obvious, indicating that the porous medium structure has good gas diffusion performance and the mass transfer control has limited effect on the reaction efficiency.

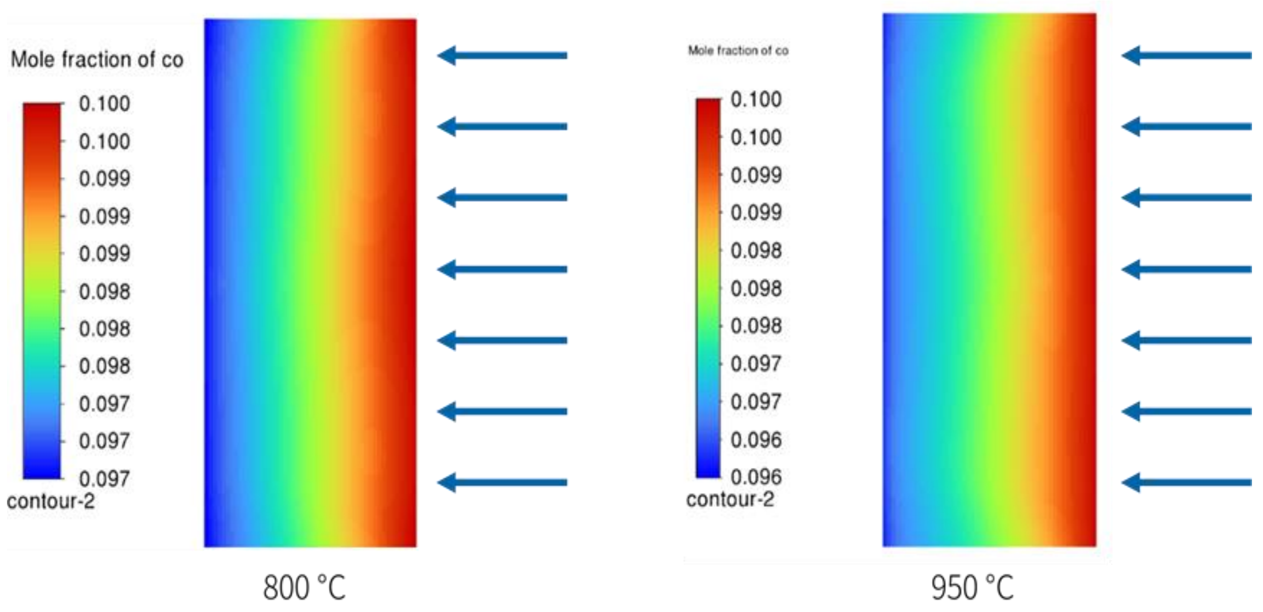

Figure 7 CO mole fraction distribution inside the sample at different temperatures when COG is used as the reducing gas

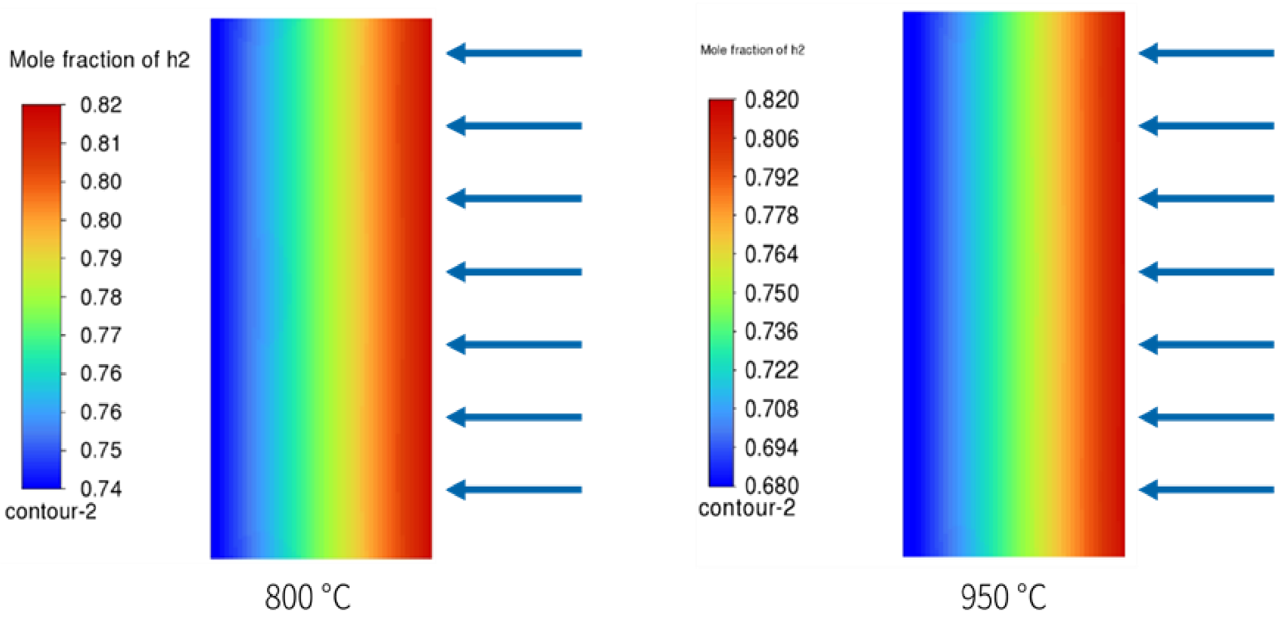

Figure 8 H2 mole fraction distribution inside the sample at different temperatures when COG is used as the reducing gas

Figure 9 shows the temperature distribution inside the pellet bed under different temperature conditions. The results show that regardless of the operating temperature of 800 ℃ or 950 ℃, the temperature difference inside the sample is always less than 0.5 K, indicating that there is no obvious hot spot or temperature gradient inside the bed. This result is related to the small size of the pellets and the uniform heating of the entire furnace. It also shows that the heat release of the reaction does not cause significant disturbances to the macroscopic temperature field.

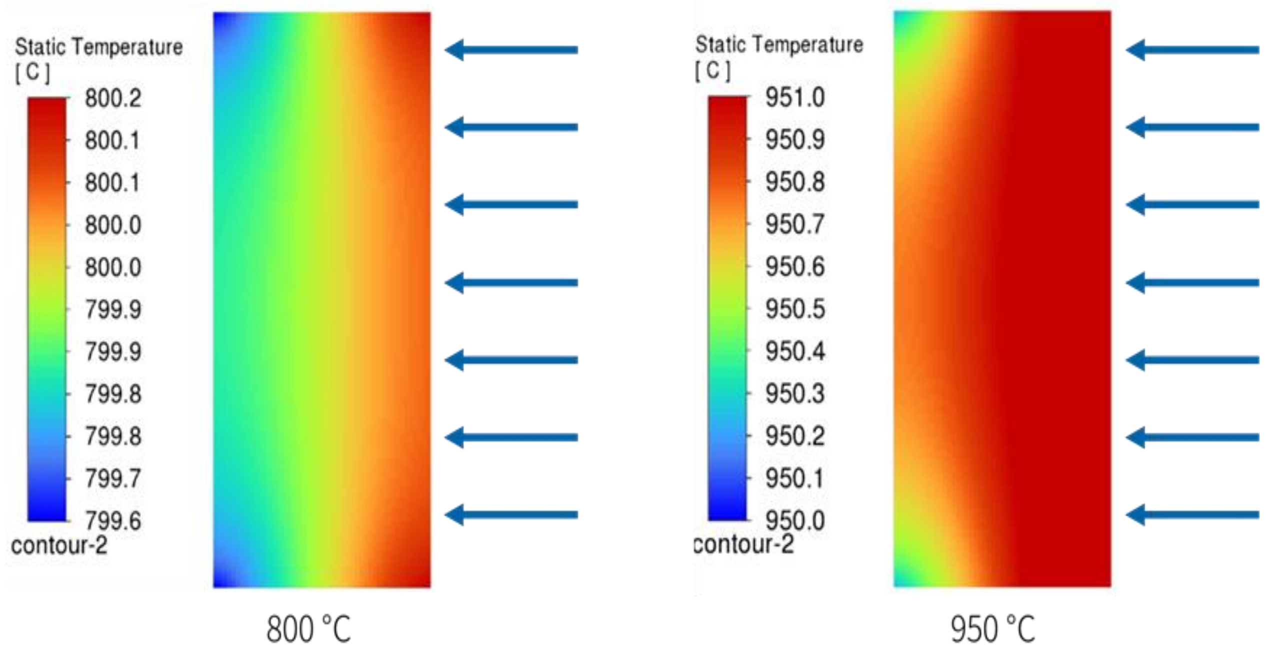

800 °C 950 °C

Figure 9 Temperature distribution inside the sample at different temperatures when COG is used as the reducing gas

5. Conclusion

This study focuses on the reduction behavior and structural evolution mechanism of iron ore pellets, and systematically evaluates the effects of different raw material properties, reducing atmosphere (especially hydrogen-rich conditions), temperature conditions, and binder types on the reduction efficiency and metallurgical properties of pellets. By introducing biomass reductants and analyzing the pore characteristics and reaction kinetics of pellets from different ore sources, the synergistic effects of factors such as porosity, reaction activation energy, and reduction starting temperature in the reduction process of pellets are revealed. The experimental results show that the use of appropriate reduction parameters and structural control methods can significantly improve the reduction degree (up to 100%), compression strength, and microstructural stability of pellets. At the same time, mathematical models are used to effectively predict the reduction kinetics and pore evolution, providing a theoretical basis and experimental basis for industrial optimization. Although this study has made initial progress in multi-source data integration and mechanism exploration, there are still certain limitations, such as the ability of some models to respond to complex atmospheres and temperature gradients needs to be improved, and the relationship between pellet microstructural changes and macroscopic properties needs to be more accurately quantified. Future research can further introduce in-situ characterization technology and multi-physics field coupling simulation to enhance the ability to predict the behavior of the entire pelletizing process and promote the industrial application of green and low-carbon reduction technology.

Acknowledgements

China Baowu Low Carbon Metallurgy Innovation Foudation-BWLCF202216

References

[1] Singh A K, Mishra B, Kumar S, et al. Reduction behaviour of iron ore pellets using hardwood biomasses as a reductant for sustainable ironmaking[J]. Biomass Conversion and Biorefinery, 2024, 14(22): 27943-27954.

[2] Das D, Anand A, Gautam S, et al. Assessment of utilization potential of biomass volatiles and biochar as a reducing agent for iron ore pellets[J]. Environmental Technology, 2024, 45(1): 158-169.

[3] Wang S, Shen F, Zheng H, et al. Isothermal Reduction and Avrami–Erofeev Kinetic Model for Reducing Iron Ore Pellets in a 70% N2–30% H2/CO Atmosphere[J]. Journal of Sustainable Metallurgy, 2024, 10(4): 2337-2351.

[4] Kittivinitchnun S, Kowitwarangkul P, Mousa E, et al. Non-Isothermal Reduction Kinetics Model of Self-Reducing Iron Ore Pellets[J]. ISIJ International, 2024, 64(10): 1503-1516.

[5] Bersenev I S, Bragin V V, Gruzdev A I, et al. Features of the iron ore pellets structure depending on the concentrate enrichment degree[J]. Steel in Translation, 2023, 53(4): 328-335.

[6] Mishra S, Mahanta J, Rath S, et al. Reduction roasting followed by pelletization study of concentrate fines of a low grade iron ore[J]. Journal of Sustainable Metallurgy, 2024, 10(2): 442-459.

[7] Hessling O, Fogelström J B, Kojola N, et al. Influence of Water Content on the Kinetics and Mechanisms of Hydrogen Reduction Using Industrial Iron Ore Pellets at 873 K–1173 K[J]. ISIJ International, 2024, 64(10): 1493-1502.

[8] Lyu B, Wang G, Xie S, et al. Effect of hydrogen-rich atmosphere on the reduction behavior and kinetics of iron-ore pellets under non-isothermal conditions[J]. JOM, 2023, 75(5): 1540-1550.

[9] Avula L S B R, Sahoo S K, Kumar M. Comparative study on reduction behaviors of low-and high-grade fired hematite iron ore pellets in coal[J]. Ironmaking & Steelmaking, 2024, 51(10): 1121-1130.

[10] Bersenev I S, Vokhmyakova I S, Ozornin N K, et al. Porosity of Iron-Ore Pellets at Different Stages of Roasting and Reduction[J]. Steel in Translation, 2023, 53(12): 1137-1143.

[11] Claremboux V, Kawatra S K. Iron ore pelletization: Part III. organic binders[J]. Mineral Processing and Extractive Metallurgy Review, 2023, 44(2): 138-154.